CONSTANT CONCENTRATION INFILTRATION MEASUREMENT TECHNIQUE: AN ANALYSIS OF ITS ACCURACY AND FIELD MEASUREMENTS

D. Bohac D. Harrje L.K. Norford

ABSTRACT

The constant concentration technique measures the air infiltration flows into each zone of a building. A detailed analysis of the control methods is performed using discrete state-space techniques and digital computer simulations. The performance of the system is improved by the use of a Kalman filter to estimate the tracer concentrations and a least squares estimation of the air infiltration flows.

The accuracy of the system is examined by measuring the airflow into a small enclosure by the constant concentration and tracer gas decay methods and a sharp edge orifice. The drift of the system is measured over a two day period. Improvements are made to the gas chromatograph to reduce the drift in the detector.

The air infiltration flows into a six zone, unoccupied, single family house are measured over a period of 11 days using the constant concentration system. These results are compared to an extensive set of decay measurements. The data display the effectiveness of the control and estimation methods in a field experiment.

INTRODUCTION

In determining the air infiltration levels in our housing stock, in many countries we are evaluating our primary sources of ventilation. In any building situation where quantification of these important air infiltration values is desired, there is a wide choice of measuring methods with an associated degree of measurement complexity and detail in the information provided (Harrje et al. 1981). Examples include single location, tracer gas decay measurements or perhaps an interpretation of pressurization information on the building, as the simplest ways to estimate air infiltration values. At the other end of the information and complexity scale are constant concentration tracer gas (CCTG) systems, which can sample each zone in the house or larger building. In addition, multiple tracer gases may be employed to document interzonal airflows to complement the individual zone air infiltration ventilation rates provided by the CCTG system.

This paper discusses the CCTG system developed at Princeton University. A detailed analysis of the control and estimation methods and resulting improvements in the operation of the system are presented. Also shown are the results of the constant concentration tracer gas measurements evaluating air exchange rates in a six zone single family house. These measurements are related to an extensive study of air infiltration in these houses using one- or two-cell tracer gas decay methods.

D.L. Bohac, D.T. Harrje, and L.K. Norford are with the Center for Energy and Environmental Studies, Princeton University, Princeton, NJ

CONTROL AND ESTIMATION ALGORITHM

The constant concentration technique measures the air infiltration flow into each zone of a building by injecting a metered amount of tracer gas to each zone so that the concentration of the tracer gas is kept at a target level in all the zones. If the tracer concentration in a zone is not near the target, the measured air infiltration rate (AIR) in that zone is in error and the air flowing from the zone causes the measured AIRs in the adjoining zones to be in error. To compute the rate of tracer injection, the control and estimation algorithm may consider the present and past level of the measured concentrations, the past injection rates, and the estimated airflow. The following section presents a detailed analysis of how to best compute the injection rate and estimate the air infiltration flow from the measured concentrations and previous injection rates.

Discrete Model and Z-plane Analysis

The first step in the analysis of a control system is to form an accurate model of the process being controlled. The coupled set of first order differential equations that govern the level of tracer gas in a multizone building is (Sinden 1978):

$$V_j \cdot \frac{dc_j}{dt} = -c_j \cdot \sum_{i=1}^{n} F_{ji} + \sum_{k=1}^{n} c_k \cdot F_{kj} + S_j \qquad (1)$$

where

V_j = volume of zone j
F_{ji} = airflow from zone j to zone i
c_j = tracer gas concentration in zone j (state variable)
S_j = rate of tracer gas injection into zone j (control)
n = number of zones in building + 1
the n^{th} zone is the outside air

This model assumes that imperfect mixing in the zone does not introduce a time lag or delay in the system.

Since the nature of the constant concentration instrumentation requires that the concentration sampling and calculation of the level of injection rate be discrete, the system is modeled with difference equations. By applying the assumptions that the tracer concentrations in the zones are near the target concentration (c_t) and that $c_n \ll c_t$, the levels of tracer gas in the j building zones are approximated by:

$$V_j \frac{dc_j}{dt} = -c_j \cdot F_{nj} + S_j \qquad (2)$$

The differential equations (2) are separate; the modeling and analysis can be carried out on one zone and applied to the rest of the zones. Integrating the approximated differential equation over the sample period yields a difference equation for the tracer concentration:

$$c_{k+1} = a_k \cdot c_k + b_k \cdot u_k \qquad (3)$$

where

c_{k+1} = concentration at time (k+1) Ts [1/1]
u_k = S_k/V (control variable- specific injection rate) [1/t]
AIR_k = F_{nk}/V (specific air infiltration rate) [1/t]
a_k = $\exp(-AIR_k \cdot Ts)$ [1/1]
b_k = $(1 - a_k)/AIR_k$ [t]
Ts = time between samples [t]
AIR_k is assumed to be constant over Ts

(dimension of variable is shown in brackets)

A complete model of the system includes the effect of uncontrolled inputs known as system disturbances. An example of a system disturbance is the flow of air from an adjoining zone that has a concentration different than the target. The equation that models the tracer concentration in the presence of disturbances is:

$$c_{k+1} = a_k c_k + b_k u_k + w_k \tag{4}$$

where

w_k is the disturbance into the system

A final addition to the system model is the equation describing concentration measurement:

$$cm_{k+1} = c_{k+1} + n_{k+1} \tag{5}$$

where

cm_{k+1} is the measured concentration
n_{k+1} is the measurement error

The measurement error is due to detector measurement errors and the nonuniformity of the concentration caused by imperfect mixing.

The analysis of the control algorithm is carried out by transforming the difference equation to state space using Z-transforms and finding the control method that gives the desired pole placement (i.e., desired response) in the Z-plane. Simulations of changes in AIR are used to verify the state-space analysis and provide a qualitative analysis of the response.

Evaluation of the Control Algorithm

To accurately measure the air infiltration flows in a building, the constant concentration measurement technique requires the level of tracer gas to remain near the target level in each zone while the air infiltration flow is changing. The criteria to meet this condition are:

1. fast response with little overshoot
2. low steady-state error
3. low sensitivity to measurement errors and disturbances (system noise)

In the state-space analysis the first two criteria translate to having the transfer function poles located near the origin in the Z-plane and the final value of c (found from the final value theorem) close to c_t. The sensitivity to system noise criterion is examined using monte carlo type simulations that include gaussian measurement errors and disturbances.

Five control methods have been proposed for the constant concentration system: proportional (P), adaptive proportional (AP), integral (I), proportional-integral (PI), and proportional-integral-derivative (PID). A simple analysis shows that the AP and PI methods provide a better system response than the P, I, and PID methods. Thus, the following discussion focuses on the AP and PI methods. The analysis is carried out in the following way:

1. The difference equation is transformed into the Z-domain to find the poles of the transfer function $H(z) = C(z)/C_t(z)$
2. Given the Z-transform of the target concentration, $C_t(z) = c_t \cdot z/(z-1)$, the final value of the concentration is found from the final value theorem.

3. The response to a ramp change in AIR from 0.2 to 0.5 h^{-1} over two hours for a gaussian measurement error and disturbance of 1% is simulated for the best control parameters. The average rms value of the deviation of the actual concentrations from the target (concentration error) and the average of the concentrations over five simulations are computed as a measure of the ability of the control to keep the concentration near the target when system noise is present.

Proportional Control. Proportional control is the simplest feedback control. For a first order system, P control provides a fast response with little or no overshoot. Its one drawback is that there is a steady state error when the control parameters (i.e., control gains and constants) are kept constant. When the control parameters are continuously updated, the steady-state error is eliminated and the speed of response is slightly decreased.

The proportional control feeds back the present error signal (the difference of the present concentration from the target concentration (c_t)) multiplied by a gain, Kp [1/t]. The expression for the control is:

$$u_k = Kp(c_t - c_k) \tag{6}$$

The difference equation for the tracer concentration is:

$$c_{k+1} = a_k \cdot c_k + b_k \cdot Kp(c_t - c_k) \tag{7}$$

The analysis of the start-up period assumes that a_k and b_k are constant and studies the response of concentration to a change in c_t. Thus, the transfer function of interest is $H(z) = C(z)/C_t(z)$. By taking the Z-transform of both sides of Equation 7 this is found to be:

$$H(z) = \frac{bKp}{(z - (a - bKp))} \tag{8}$$

The one pole (value of z that sets the denominator equal to zero) is located at (a - bKp) and can be placed at zero by setting Kp = a/b. Given that $c_t(k)$ is a step change from 0 to c_t, the final value (c_f) of c(k) is:

$$c_f = \lim_{z \to 1} C(z) \cdot (z-1) = \lim_{z \to 1} \frac{(z-1) \cdot c_t \cdot bKp}{(z-1)(z-(a-bKp))} \tag{9}$$

$$c_f = (c_t \cdot bKp)/(1-a+bKp)$$

Note that the final value is less than c_t and approaches c_t as Kp increases.

The simulation in Figure 1 shows the concentration and control response to a step in AIR from 0.2 to 0.5 h^{-1} (Ts= 4 minutes and c_t= 100) for Kp = a/b. The normalized control values shown in the graph are defined as u_k/c_t and are equal to AIR_k when the concentration is kept at the target level. As predicted by the state-space analysis, the control response is fast with no overshoot and the steady state concentration is below the target.

The error in the final concentration does not have to be as large as the analysis indicates. The value of Kp could be increased to decrease the error. However, this would cause an oscillatory system response and would not eliminate the error. The target concentration can be reached exactly by replacing the parameter c_t in the control equation (6) with a larger value that is dependent on the level of AIR and the sample time. By introducing this new parameter, the control equation is changed to:

$$u_k = Kp(c_o - c_k) \tag{10}$$

where

c_o is the new parameter in the error signal

By replacing c_t with c_o and c_f with c_t in the final value equation, the value of c_o that sets the final value equal to the target found is to be:

$$c_o = c_t \cdot (1-a+bKp)/bKp \tag{11}$$

The substitution of c_t with c_o has the effect of feeding back information about the AIR into the control equation. Because c_o is dependent on the level of the AIR (via the parameters a and b) it is necessary to use the measured AIR to compute the value of c_o for $c_f=c_t$. This method (an example of adaptive control) responds properly when the measured AIR is not greatly different than the true AIR. For slowly changing AIRs, the measured AIR is within 10% of the true AIR and the concentration error is less than 1%. However, the method of estimating the AIR by dividing the injection rate summed over a period of time by the desired concentration (discussed below) does not respond quickly to sudden changes in AIR. Figure 2 displays the simulated concentration and control response to a step change in AIR from 0.2 to 0.5 h^{-1} for proportional adaptive control. Because of the lag in the estimation of the AIR, there is a lag in the concentration reaching the target level. In addition, the control value overshoots the steady level for a period of time equal to the amount of time the injection rate is summed (in this case 40 minutes). This causes the estimate of the AIR to be high and, in turn, the concentration to overshoot the target a small amount. Because of the lag in estimating the AIR, the proportional adaptive method is slightly oscillatory.

Errors in the measurement of the concentration decrease the system's ability to keep the concentration at the target level. To explore this issue quantitively, a gaussian measurement error and disturbance of 1% is introduced into the simulation of the system response to a ramp change in AIR. Over five simulations the average rms concentration error is 1.63 and the average concentration is 99.74. As expected, the average concentration is below the target because of the lag in the estimation of AIR. Also, the concentration error is significantly larger than the magnitude of the disturbance. These values obtained for the AP method will be compared to those of the PI method to compare the sensitivity of the control methods to system noise.

Proportional-Integral Control. Proportional-integral control is a combination of proportional and integral terms. The addition of the integral term to the proportional term eliminates the final concentration error of proportional control and the need for adaptive control. When broken into parts, the proportional term can be thought of as providing the amount of control needed to bring the concentration from the measured to the target level, and the integral term adds an amount needed to counteract the drop in concentration that would result from air infiltration. By properly choosing the control gains, the system response to changes in AIRs is a one-step delay with no overshoot. Thus, PI control satisfies the two response criteria of a fast response with no overshoot and no steady-state error.

The PI method feeds back the error signal multiplied by Kp [1/t] added to the integral of the error signal multiplied by Ki [$1/t^2$]. The expression for the control is:

$$u_{k+1} = u_k + (Kp + KiTs)(c_t - c_{k+1}) - Kp(c_t - c_k) \tag{12}$$

And the transfer function is:

$$H(z) = \frac{bz(Kp + KiTs) - bKp}{(z - 1)(z - a) + bz(Kp + KiTs) - bKp} \tag{13}$$

There is one choice for Kp and Ki that places both poles at the origin: Kp = a/b and Ki = 1/(bTs).

Given a step change in $c_t(k)$ from 0 to c_t the final value of c(k) is:

$$c_f = \lim_{z \to 1} \frac{c_t \cdot z(z - 1)[bz(Kp + KiTs) - bKp]}{(z-1)[(z-1)(z-a) + bz(Kp + KiTs) - bKp]} \qquad (14)$$

$$= c_t$$

The addition of the integral term to the proportional term has eliminated the error in the final concentration for all values of Kp, Ki, and Ts.

The simulation in Figure 3 shows the concentration and control response to a step in AIR from 0.2 to 0.5 h^{-1} (Ts= 4 minutes and c_t= 100) for Kp and Ki equal to a/b and 1/bTs. As predicted from the state-space analysis, the response displays a one-step delay in reaching the concentration and control equilibrium. This occurs because an increase in AIR decreases the concentration, which causes an increase in the integral of the error signal (i.e., the amount of control needed to counteract air infiltration). By choosing the proper values of Kp and Ki, the control is increased enough to bring the concentration to the target level in the next sample period, and the control is kept at the level required to hold the concentration at the target.

The system noise sensitivity analysis was conducted for the PI method. Over five simulations the average rms concentration error is 2.36 and the average concentration is 100.84. The deviation is larger than that of AP and average concentration above the target is due to the system responding quickly to any deviations of the concentration from the target and the limitation of not allowing negative control values (which would correspond to removing tracer gas).

Comparison of the Control Methods. System response for integral and PID control is not as good as that of AP and PI control. The integral method is not acceptable because of the long settling time of the response. The addition of a derivative term to the PI control does not improve the system response and the derivative term is sensitive to noise.

AP and PI control provide fast system response with little or no overshoot and no steady state error. The difference between the two controls is that the AIR feedback for AP is indirect while PI has direct feedback. AP control adjusts the level of control for varying AIRs by changing the magnitude of the control parameter, c_o. The lag in the estimation of AIR introduces a time lag in the system. This causes concentrations to be, on the average, below the target for increasing AIRs and above the target for decreasing AIRs. For PI control the integral term directly compensates for the level of AIR. This method has the drawback of being sensitive to measurement errors. The sensitivity of the control and the restriction on negative injection rates cause concentrations to be above the target. Because the error in concentration for both controls has approximately the same magnitude, the selection of a best control requires further evaluation.

The following sections present two techniques for improving the response of the AP and PI methods in the presence of noise. These techniques attempt to increase the accuracy of the estimated concentration and AIR and reduce the lag in the estimate of AIR.

Concentration Estimation

A Kalman filter is a method of estimating the concentration so that the variance in the estimated concentration ($\bar{c}$) from the true concentration is minimized. This is accomplished by properly computing the estimation gain (Ke_k) used to combine the measured concentration ($\hat{c}$) and concentration extrapolated from the difference equation (c^*) to form an estimation of the true concentration:

$$\bar{c} = c^* + Ke_k(\hat{c} - c^*) \qquad (15)$$

Ke_k is computed by considering the covariance of the past estimate of the concentration (P_k), the covariance of the disturbance into the system (Q_k), and the covariance of the measurement error (R_k). The equations for the computation of Ke and the estimated concentration are displayed in Table 1. In brief, extrapolation Equations 16 and 17 are derived by finding the expected values of c_k and $(\bar{c}_k - c_k)^2$ from the tracer gas difference Equation 4. The following three equations, 18 to 20, are equivalent to a recursive least squares estimator. A complete derivation of these equations may be found in any text on optimal estimation. The references (Franklin and Powell 1980; Gelb 1974; Bryson and Ho 1975) have been used by the author for the presentation of the equations in Table 1.

The steady-state value of Ke can be derived as an explicit function of a^2, Q, and R. First, the steady-state value of P is found by substituting $P_{k+1}(-)$ from Equation 17 into Equation 18 and setting $P_k(+)$ equal to $P_{k+1}(+)$. The steady-state value of Ke is then found by dividing P(+) by R:

$$Ke = \frac{(a^2 - 1) - Q/R + \sqrt{((a^2 - 1) - Q/R)^2 + 4(Q/R)a^2}}{2a^2} \qquad (21)$$

This equation shows that Ke is an explicit function of a^2 and the ratio of Q/R. The information needed for the computation of Ke is simply the relative magnitudes of Q and R and the value of a.

The above analysis of the Kalman filter has assumed that the disturbance and measurement errors are known and/or measurable. Unfortunately, for most structures these values are difficult to obtain. Measurement errors depend on the error in the detector and the uniformity of the concentration in the zone. The precision of the detector can be quantified and is approximately less than or equal to 1% of the measured value for the system in use. However, the uniformity of the concentration in the zone will be dependent on the strength and direction of airflow in the zone (intrazone flow) and the rate of infiltration flow (i.e., larger AIRs will cause greater dilution near the exterior envelope). Since the natural intrazone flow can show large fluctuations and is usually too low to provide adequate mixing (Collet 1981; Lundin and Blomsterberg 1983; Alexander et al. 1980), small fans are placed in the room to accelerate the diffusion of the injected tracer gas and increase mixing. With a mixing fan present, the only parameter causing changes in the measurement error is the level of AIR. The measurement of the covariance of the measurement error for the operation of the constant concentration system in a multizone building is a subject of future research.

The second value required for the computation of Ke is the covariance of the disturbance. The disturbance input to a zone is a result of the flow of air from an adjoining zone that has a concentration different than the target. Since it is not possible to measure the flow rate and concentration of each airstream entering and leaving a zone, it is not possible to directly measure the covariance of the disturbance input. Developing a procedure to measure and measuring Q in a single zone is also the subject of future research.

Because the values of Q and R are not presently well known for the constant concentration system, it is important to understand the sensitivity of the estimation covariance to nonoptimal values of Ke. To measure the sensitivity of P to suboptimal values of Ke, a series of simulation trials is conducted for a constant ratio Q/R and Ke varying from 0 to 1 in increments of 0.05. Each simulation trial is carried out over 2000 minutes, for Ts = 4 minutes, the AIR steady at 0.4 h^{-1}, and constant values of Q, R, and Ke. The covariance of the estimate is computed from the variance between the estimated and true concentration. The results of these simulation trials for Q/R equal to 1, 0.2, and 5 are displayed in Figure 4 - note that the value of P has been normalized by dividing by R. The results of the simulation closely agree with the expected results:

1. The estimate covariance is equal to R for Ke = 1.0

2. The value of Ke for minimum P (Ke_{ss}) is equal to the value given by Equation 21

When the chosen value of Ke is within approximately 0.2 of Ke_{ss}, the estimate covariance is only slightly increased above the minimum, but deviations of Ke 0.2 or more below Ke_{ss} cause a large increase in P. Figure 5 also shows that using a Kalman filter with an optimal gain significantly reduces the value of P from that obtained by measurement only (Ke = 1.0) and that the reduction in P increases as Q/R decreases. For example, the reduction in P for Q/R = 5 is 15% and that for Q/R = 0.2 is 65%.

Air Infiltration Rate Estimation

The estimated specific air infiltration rate is used for three purposes: (1) the reported value of the outdoor airflow rate into the zone is equal to the AIR multiplied by the zone volume, (2) the AIR is used in the process of estimating the concentration, and (3) the AIR is used by the proportional adapative control method to compute c_o. Thus, any error in the estimated AIR not only causes incorrect values of the reported infiltration flow rate but also affects the control of the system. The averaging, modified averaging, and weighted least squares (WLS) methods of AIR estimation are discussed in this section.

The averaging method computes an estimate of the average infiltration flow rate by dividing the tracer injection rate averaged over a period of time ($\bar{S}$) by the target concentration:

$$F_{nj} = \frac{\bar{S}_j}{c_t} \tag{22}$$

The assumption is made in the derivation of the averaging method that the concentration is held constant at the target level. Although the averaging method provides a fairly accurate estimation of the AIR (Sandberg 1985), in general, neglecting changes in the concentration decreases the accuracy of the AIR estimation.

The averaging method can be modified to include the information of the deviation of the concentration from the target. By including the normalized difference in the concentration and using the average concentration ($\bar{c}$) instead of c_t, the modified averaging equation is found to be:

$$F_{nj} = \frac{\bar{S}}{\bar{c}} + \frac{V[c_{k-p} - c_k]/Ta}{\bar{c}} \tag{23}$$

The plot in Figure 5 displays the values of AIR estimated by the averaging and modified averaging methods at each sample time when there is a step change in the true AIR from 0.2 to 0.5 h^{-1} [Ts = 4 minutes, measurement error = system disturbance = 0.7% of the target concentration, Ta = 10Ts]. This figure shows that the modified averaging method is more accurate than the averaging method in estimating the average AIR.

Using the concentration difference Equation 3 as a model, the WLS method computes an estimate of a and b that best fits the time history data of the control and concentration values. The estimated values of a and b are then used to calculate the estimated value of the AIR. Because the difference equation is derived directly from the concentration differential equation, there are no inherent inaccuracies in the WLS method. Thus, the accuracy of the WLS estimate is only a function of the magnitude of the measurement error and accuracy of the system model.

The concentration is not measured accurately enough to provide an accurate estimate of the AIR over one sample time. Thus, a series of observations are used to estimate the parameters a and b in the estimation interval. For a series of n observations, the following matrix equation is formed:

$$C_{n+1} = [C_n \quad U_n] \; P = H \; P \tag{24}$$

where

C_{n+1} is a nx1 vector equal to
$[c_{k+1} \quad c_{k+2} \quad \cdot \cdot \quad c_{k+n} \quad c_{k+n+1}]^T$

H is a nx2 observation matrix equal to
$[[c_k \quad c_{k+1} \quad \cdot \cdot \quad c_{k+n}]^T \quad [u_k \quad u_{k+1} \quad \cdot \cdot \quad u_{k+n}]^T]$

P is a 2x1 parameter matrix equal to $[a \; b]^T$

Given the n observations of the control and concentration values, this matrix equation is used to estimate the parameter matrix. The least squares estimation process computes an estimate of the parameters that minimizes the squared error in the estimated future concentration:

$[C_{n+1} - H P]^T [C_{n+1} - H P]$. By taking the derivative of the squared error with respect to the estimated parameter matrix, the value of P for the minimum squared error is found to be:

$$P = (H^T H)^{-1} H^T C_{n+1} \tag{25}$$

The plot in Figure 6 displays the values of AIR estimated by the modified averaging and least squares methods at each sample time when there is a step change in the true AIR from 0.2 to 0.5 [Ts = 4 minutes, measurement error = system disturbance = 0.7% of the target concentration, Ta = 10Ts]. This plot shows that the estimated average AIR computed by the least squares method is nearly equivalent to the value computed by the modified averaging method. The analysis of the error of the estimated average AIR in the presence of system noise and when the AIR is changing leads to the following general conclusions:

1. The modified averaging method is significantly more accurate than the averaging method.

2. Except at high levels of measurement error, the accuracy of the modified averaging and least squares methods are nearly equivalent.

3. For disturbances less than 1.5% and measurement errors less than 3%, the least squares and modified averaging methods estimate the average AIR within approximately 5% of the average AIR.

Although one of the purposes of AIR estimation is to provide an accurate estimate of the average AIR during a period of time, the value used for the control computation should be more representative of the present AIR. The least squares method can provide a more accurate estimate of the present AIR by giving a heavier weight to the most recent observations. The weighting of the observations is obtained by including a diagonal weighting matrix (W) in the matrix equation for the squared error of the estimated future concentration:

$$error_2 = [C_{n+1} - H P]^T W [C_{n+1} - H P] \tag{26}$$

By taking the derivative of Equation 25 with respect to the estimated parameter matrix, the value of P is computed as:

$$P = (H^T W H)^{-1} H^T W C_{n+1} \tag{27}$$

The weighting given to each term is defined as w(k). Franklin and Powell (1980) present $w(k) = (1 - gm)gm^{(n-k)}$ as a commonly used function, which weights the most recent observations more than the past. For small values of gm the recent observations are weighted much more heavily than the past values, which allows the estimate to respond quickly to changes in the AIR but cause it to be susceptible to measurement errors. As gm approaches 1.0, each term is given equal weight, which decreases the sensitivity to measurement errors.

The plot in Figure 6 also displays the values of AIR estimated by the weighted least squares (gm = 0.8) method for a step change in the true AIR. This plot shows that the weighted least squares method responds much faster than the other two methods to the sudden change in AIR. The only drawback to using lower values of gm is that the estimate places the majority of the weight on a small number of observations. The analysis of the error of the estimated present AIR, when the AIR is changing and there is system noise present, leads to the following general conclusions:

1. The modified averaging method is significantly better than the averaging method.

2. Except at high levels of system disturbance, the weighted least squares method is significantly better than the modified averaging method.

3. The value of gm for minimum estimate error decreases with increasing AIR rate of change and increases for increasing measurement error and system disturbance.

4. Values of gm of 0.8 and below are only useful for abrupt changes in the AIR, small measurement errors, and small disturbances.

5. Over the range of variables studied, the values of gm equal to 0.90 and 0.95 provide the most accurate estimate of the AIR.

Performance Improvement

The preceding sections show that the error in the estimation of the concentration and AIR is improved through the use of a Kalman filter and WLS estimation. However, it is even more important to quantify the improvement in the ability of the system to keep the actual concentration near the target when the AIR is changing and there is noise in the system. This is achieved by repeating the system noise sensitivity analysis for the system operating with a Kalman filter and WLS estimation. Ke = 0.6 and gm = 0.9 are used for the series of simulations.

Table 2 displays the results of the sensitivity analysis. These results show that the concentration error decreased by 3% for the AP method and by 33% for the PI method. Also, the average concentration stayed nearly the same for the AP method while that for the PI method moved from being significantly above to nearly at the target level. The positive results for the PI method are due to the improvement in the estimation of the concentration, which increased the accuracy of estimating the proportional and integral terms. Better estimation of these terms reduced the large fluctuations in the control which reduced the number of times the system needed a negative control value.

The improvement is not as significant for the AP control. This is because the extrapolated concentration does not indicate the change in the AIR as quickly as the measured value does (the extrapolated value is calculated from an estimated AIR, which has a lag in it, while the measured value is directly affected by the actual AIR). Thus, the improvement in the performance gained by a more accurate estimate of the concentration and a faster response in the estimation of the AIR is negated by the addition of the lag in the Kalman filter. However, in comparison to the integral term for the PI method, using the estimated AIR to compensate for variations in the AIR provides a more accurate estimate of the injection rate. This is displayed by the lower deviation for the adaptive method - 13% lower than the PI method. Because of the lower concentration deviation, the adaptive proportional method is chosen as the preferred method for the CCTG system.

LABORATORY EXPERIMENTS

The constant concentration tracer gas sytem is a relatively complex instrument. Stable operation and accurate measurements depend on the design of the control algorithm and the stability and accuracy of the components in the system. Although much care is taken in the calibration and design of the separate components, it is important to study the accuracy of the entire system. This has been done by comparing the measurements obtained by the CCTG system of the airflow into a small enclosure to those by the tracer decay method and flow through a sharp edge orifice. In addition, the drift of the system is measured over a two day period.

CCTG System Description

Figure 7 displays a schematic of the constant concentration tracer gas system developed at Princeton University. The system consists of an electron capture gas chromatograph, a series of ten sample and injection lines, an auxiliary pump, valve control electronics, and a microcomputer data acquision system. A detailed description of the components in the CCTG is found in Bohac and Harrje (1985) and a description of the calibration procedures is found in Harrje et al. (1984). The system operates on a 60-second cycle during which the following procedures take place:

1. The concentration of the zone is measured.
2. The sample valve of the next zone is opened.
3. The estimated concentration, AIR, and injection rate are computed.
4. This new information is displayed on the monitor and saved to a disk file.
5. Tracer gas is injected into all the zones.

The concentration measurement takes approximately 30 seconds to complete and is followed by procedures (2) to (4) which require a few tenths of a second. This leaves 30 seconds for the injection of tracer gas. After the cycle is complete, the system repeats the procedures on the next zone. When the procedures have been performed on all the zones the process begins again at the first zone. Thus, the length of time between samples in a zone is equal to the product of the cycle time (one minute) and the number of zones. It is important to note that, instead of performing only one injection in a zone between samples, the system injects a pulse of tracer gas into every zone during each 60 second cycle. This method more closely approximates constant injection. For each zone the measured concentration, computed injection rate, and estimated present AIR at each sample time are stored in a disk file. At the end of each hour of operation the average and standard deviation of the measured concentration and the estimated average AIR are stored to a separate hourly data disk file.

Flow Measurement Comparison

The experiments are conducted using a 59" (1.50 m) x 92" (2.34 m) x 95.5" (2.43 m) tightly sealed enclosure located in a building. Air is brought in by a blower and duct system from the side of the building through a sharp edge orifice and into the bottom of the enclosure. Another blower and duct system exhuasts the air from the top of the enclosure to the roof of the building. Mixing is provided by two small fans. SF_6 is injected near the air entry point and sampled from three locations at mid-height of the enclosure. An error analysis shows that the accuracy of the sharp edge orifice/inclined manometer instrument is 1.5 to 2.5% and that of the tracer decay method is 2 to 4%. Given the accuracy of the calibration gas, injection system, SF_6 detector, and estimation method, the accuracy of the CCTG system is expected to be 2 to 5%.

Numerous decay and constant concentration trials were performed for high-flow and low-flow conditions. Table 3 displays the results of these trials. For the low-flow condition there is a 5.3% difference between the CCTG and decay measurements and a 4.0% difference between the CCTG and orifice measurements. For the high-flow condition there is a 0.4% difference between the CCTG and decay measurements. Thus, the difference between the measurements of the methods falls within the expected accuracy of the CCTG system.

Drift Measurement

The CCTG system is designed to operate continuously for more than a week. In order to accomplish this design goal, a number of modifications were made to the commercial SF_6 detector. These modifications are:

1. Elimination of unnecessary valves and connections to reduce the possibilty of leaks.

2. The voltage output is shielded, buffered, and sent through a low-pass filter to reduce noise and effect of the impedance of the voltage measuring device.

3. The sample and detection loops are decoupled to eliminate the effect of the backround SF_6 concentration.

The magnitude of the drift of the system is analyzed by measuring the airflow in the enclosure using the CCTG system and orifice over two days. The results of this experiment are displayed in Figure 8 and show that there is no systematic drift and that the deviations of the measurements are small. In fact, the deviation in the airflow measured by the CCTG system (1.2% of the average value) is only slightly larger than that of the orifice (0.9% of the average value). In relation to the system accuracy of 2 to 5% this is an acceptable amount of drift.

FIELD EXPERIMENTS

For more than two years, a series of detailed air infiltration measurements have been conducted over the complete yearly weather cycle on two identical side-by-side test houses in Gaithersburg, Maryland. These measurements have been part of a broad study of the interaction of air infiltration, indoor air quality, and energy in tightly constructed, well-insulated homes. The standard method of collecting air infiltration data throughout the study has been tracer gas decay. Operation of the duct air circulation fans has transformed each house into a single well-mixed cell. Natural air mixing in the upper and lower floors, with the fan operated occasionally, results in two-cell behavior. The present phase of the air infiltration portion of the study has been to use constant concentration tracer gas equipment to study the air infiltration in six individual zones. This has allowed comparisons between the two methods as well as looking at the air infiltration profile in a much more detailed way.

The Experimental Houses

The bi-level houses used in this study were built during the fall of 1982 as part of a new subdivision approximately 22 miles (35 kilometers) northwest of Washington, DC, in Gaithersburg, Maryland. Two identical houses were constructed to somewhat relaxed building standards so that later retrofitting efforts could be made to improve the tightness of the building envelope. One of the houses, the experimental house, was subsequently retrofitted to achieve six air changes per hour (ACH) leakage rate at 0.2 inches of water (50 pascals) differential pressure, whereas the control house remained at ten ACH at 0.2 inches of water (50 Pa) throughout the period of testing.

The house floor plan is shown in Figure 9 indicating floor area and volumes. One path of communication between the various rooms and floors is the duct system that is used to distribute conditioned air in the heating and cooling seasons and can be operated continuously or intermittently ("auto setting"). Further details of the various aspects of the research conducted in these houses can be found in (Nagda et al. 1983; Harrje et al. 1983; Nagda et al. 1984; Koontz and Nagda 1984; Nagda et al 1985).

Deployment of the CCTG System

To insure proper operation of the CCTG system, the division of the building into separate zones and the placement of the injection and sampling systems must be done in a logical and consistent manner. The building is divided into separate zones where significant physical boundaries exist (i.e. walls and floors) and where it can be assured that the air in each zone can be well mixed with one or two mixing fans. As Figure 9 points out, six zones were assigned in the upper and lower levels of the house. Each of the six zones contained one sulphur hexafluoride tracer gas injection point (centrally fed by a plastic tube) located close to a small mixing fan necessary to circulate the air within that zone. Sampling in the smaller volume zones required only single sampling locations (as shown), whereas the larger zones such as the living/dining room and kitchen zone (zone 5), and the basement (zone 6) required multiple point sampling. In each case, a single 1/8 inch (3.2 mm) diameter plastic tube was used to convey the zone air sample from the particular zone to the central control point of the CCTG system, but in the larger zones the tubing branched out to multiple sampling point locations. An additional fan was used in the larger zone (5) as noted in Figure 9.

Successful operation of the CCTG system is determined from its ability to maintain tracer gas concentrations within narrow bounds of the target concentration. The six zones were

sampled every six minutes throughout each hour. Figure 10 displays the quartile values of the hourly AIR, average concentration, and standard deviation of the concentration for the six zones and the whole house over the 11 days of tests. The hourly average concentration data indicate that the average concentration was within 1% of the target at least 50% of the time. The standard deviation of the concentration in the upstairs zones varies from 0.8 to 10 ppb with a median of approximately 3.6 ppb or 2.4% of the target. The deviation in the basement varied from 1 to 15 ppb with a median of 4.7 ppb or 3.1% of the target. These results are similar to those obtained by other systems (Lundin and Blomsterberg, 1983; Collet, 1981) and indicate that the system was operating properly.

AI Rates in the Upper and Lower Floors of the Control House

The original SF_6 decay data establish typical upper and lower floor air infiltration rates that change noticeably (see Figure 11) when the air circulation fan switches from periodic to continuous operation. Using the same specified weather conditions, but for a much narrower range of values, hourly data from the CCTG measurements have been used to form a similar average air exchange rate schematic for the upper and lower floors of the control house. Although the house average rates are similar to the original data, there are changes in the distribution. When the fan operated continuously, the upper level air infiltration rates increased from 0.12 to 0.21 h^{-1} in comparison to periodic operation, and, correspondingly, the basement AI rates decrease from 0.90 to 0.46 h^{-1}. Thus, when the fan ran continuously, the CCTG system was found to be capable of measuring differences in zonal air exchange rates, although these differences were reduced from the case when the fan was used periodically. This is in contrast to the tracer gas decay method where differences in the air infiltration rate between the upstairs and downstairs could not be measured when the fan operated continuously.

Perhaps the most dramatic illustration of the variations in air infiltration rates of the upper versus lower floor and individual zones is found by plotting the air exchange over days of testing as shown in Figure 12. Variation between upper floor zones is of the order of 1 to 1, ranging to 5 to 1, and between the lower and upper floors is as great as 10 to 1. Air exchange rates below 0.1 ACH are repeatedly shown to take place in many of the upper floor zones over the test period illustrated. This is best seen when the bedroom zones are plotted separately in Figure 13.

Wind Direction

The CCTG data just discussed will now be reviewed for a case where adequate data points were available to allow discrimination between wind speed and direction over an extended range of wind speeds, as shown in Figure 14. Here the two sets of data points are for wind flowing from the direction of the neighboring experimental house vs. wind from all other directions. In the first data set, additional wind protection would be anticipated for the control house because of wind blockage by the experimental house and because the wind is impinging on the garage side of the control house (i.e., protecting the basement zone). Clearly the data indicate there is a wind directional effect; the average air infiltration drops in the control house for winds from that shielded direction, and the coefficient of determination (R^2) for the wind data from other directions is improved (R^2 increased to 0.8 from 0.66).

Spot checks were made of how wind direction (matching wind speed and temperature difference) can affect individual zone air exchange rates. For example, a 10.1 m/h (4.5 m/s) wind impinging on zone (5) raised the 0.14 AI rate to 0.33 ACH. At the same time the AI rate in zone (2) on the leeward side of the house dropped from 0.22 to 0.05 ACH. This is given as a typical example of what air infiltration changes can take place as a result of wind direction and that such changes should be of concern when considering whether or not individual room ventilation rates are being met. Ventilation adequacy and ventilation standards are further discussed in Harrje and Janssen (1985), using the seasonal variations in air infiltration that have been documented in this research.

CONCLUSION

1. Monte Carlo type simulations show that when the AIR is changing and system noise is present the incorporation of a Kalman filter and weighted least squares estimator improved the operation of the system.

2. Laboratory experiments show that over an extended period of time, the CCTG system accurately measures the air infiltration flow into an enclosure.

3. The field test of the CCTG system indicated that the system operated properly and yielded additional air infiltration information on: individual zone variations, upstairs/downstairs variations, and wind effects. These added ventilation rate details provide further data on influences of weather and house system functions and thus prove useful in analyzing the impact on indoor air quality and energy.

REFERENCES

Alexander, D.K.; Etheridge, D.W.; and Gale, R. 1980. "Experimental techniques for ventilation research" In First air infiltration centre conference: Air infiltration instrumentation and measuring techniques. Air Infiltration Centre Document AIC-PROC-1-80, pp. 45-71.

Bohac, D.L., and Harrje, D.T. 1985. "The accuracy of constant concentration tracer gas measurements" 6th AIC Conference - Ventilation stratagies and measurement techniques, Air Infiltration Centre Document AIC-PROC-13-85.

Bryson, A.E., and Ho, Y. 1975. Applied optimal control. Washington D.C.: Hemisphere Publishing Corp.

Collet, P.F. 1981. "Continuous measurements of air infiltration in occupied dwellings." In Second air infiltration centre conference: Building design for minimum air infiltration, Air Infiltration Centre Document AIC-PROC-2-81, pp. 147-160.

Franklin, G.F., and Powell, J.D. 1980. Digital control of dynamic systems. Reading, Mass.: Addison-Wesley.

Gelb, A. 1974. Applied optimal estimation. Cambridge: M.I.T. Press.

Harrje, D.T.; Grot, R.A.; and Grimsrud, D.T. 1981. "Air infiltration: Site measurement techniques" 2nd AIC conference proceedings - Building design for minimum air infiltration. Air Infiltration Centre, Document AIC-PRO-2-81, pp. 113-133.

Harrje, D.T.; Nagda, N.L.; and Koontz, M.D. 1983. "Air infiltration, energy use, and indoor air quality - How are they related." Air infiltration review, Vol. 5, No. 1, November 1983.

Harrje, D.T., and Janssen, J.E. 1984. "A standard for minimum ventilation" 5th AIC Conference Proceedings - The implementation and effectiveness of air infiltration Standards in buildings. Air Infiltration Centre, Great Britian, Document AIC-PROC-5-84, pp. 3.1-3.16.

Harrje, D.T.; Dutt, G.S.; Bohac, D.L.; and Gadsby, K.J. 1985. "Documenting air movements and infiltration in multi-cell buildings using various tracer techniques." ASHRAE Transactions, Vol. 91 Part 2.

Koontz, M.D., and Nagda, N.L. 1984. "Infiltration and air quality in well-insulated homes: 3 - Measurement and modeling of pollutant levels." IBID, pp. 511-516.

Lundin, L., and Blomsterberg, A. 1983. "An automated air infiltration measurement system - Its design and capabilities, preliminary experimental results." Air Infiltration Review, Vol. 4, No. 1, pp. 8-10.

Nagda, N.L.; Koontz, M.D.; Rector, H.E.; Harrje, D.T.; Lannus, A.; Patterson, R.M.; and Purcell, G.G. 1983. "Study design to relate residential energy use, air infiltration, and indoor air quality." Proceedings of the 76th Annual Air Pollution Control Association Meeting, Paper No. 83-29.3.

Nagda, N.L.; Koontz, M.D.; and Karpay, B. 1984. "Infiltration and air quality in well-insulated homes: 2 - Effect of conservation measures on air exchange and energy use." Proceedings of the 3rd International Conf. on Indoor Air Quality and Climate, Swedish Council for Building Research Document D20:84, Vol. 5, pp.165-170.

Nagda, N.L.; Harrje, D.T.; Koontz, M.D.; and Purcell, G.G. 1985. "A detailed investigation of the air infiltration of two houses." ASTM Proceedings of Conference on Measured Air Leakage Performance of Buildings, ASTM.

Nagda, N.L.; Koontz, M.D.; and Rector, H.E. 1985. "Energy use, infiltration, and indoor air quality in tight, well-insulated residences." Final Rpt. EPRI RP2034-1, GEOMET Technologies, Report ERF-1461, March.

Sandberg, M., and Blomquist, C. 1985. "A quantitative estimate of the accuracy of tracer gas methods for the determination of ventilation flow rate in buildings." ASHRAE Transactions, Vol. 91, Part 2.

Sinden, F.W. 1978. "Multi-chamber theory of air infiltration", Building and Environment, Vol. 13, pp. 21-28.

BIBLIOGRAPHY

Bohac, D.L. 1985. "The use of a constant-concentration tracer gas system to measure ventilation in buildings." Master's thesis, Princeton University, Department of Mechanical and Aerospace Engineering.

ACKNOWLEDGMENTS

The study in the GEOMET research houses in Gaithersburg, MD, is supported by the Electric Power Research Institute under Contract Number RP 2034-1. The development of the Princeton University Constant Concentration Tracer Gas System is supported by the U.S. Department of Energy under Contract Number DE-AC02-77CS20062.A017.

The authors also wish to acknowledge the contributions of Michael Koontz of GEOMET for his work on the original air infiltration data using tracer gas decay. We also wish to acknowledge the contributions of Kenneth Gadsby of Princeton University in the development of the CCTG system and the deployment in the control house.

TABLE 1

Kalman Filter Equations

Concentration Extrapolation

$$c^*_{k+1} = a_k c_k + b_k u_k \tag{16}$$

Concentration Covariance Extrapolation

$$P_{k+1}(-) = a_k^2 \cdot P_k(+) + Q_k \tag{17}$$

Concentration Covariance Update

$$P_{k+1}(+) = 1/[1/P_{k+1}(-) + 1/R_{k+1}] \tag{18}$$

$$= [R_{k+1}P_{k+1}(-)]/[R_{k+1} + P_{k+1}(-)]$$

Estimation Gain Computation

$$Ke_{k+1} = P_{k+1}(-)/[P_{k+1}(-) + R_{k+1}] \tag{19}$$

$$= P_{k+1}(+)/R_{k+1}$$

Concentration Estimation

$$\bar{c}_{k+1} = c^*_{k+1} + Ke_{k+1}(\hat{c}_{k+1} - c^*_{k+1}) \tag{20}$$

Notation:
- $\bar{c}_*$ - estimated concentration
- c^* - extrapolated concentration
- $\hat{c}$ - measured concentration
- n - measurement error
- w - disturbance input
- P(-) - covariance of the concentration before being updated by the present measurement
- P(+) - covariance of the concentration after the update

Assumptions in the derivation:

"white noise", gaussian zero mean disturbance -

$$E[w_k] = 0, \quad E[w_k w_l] = 0, \quad E[w_k^2] = Q_k$$

"white noise", gaussian zero mean measurement error not correlated with the disturbance -

$$E[n_k] = 0, \quad E[n_k n_l] = 0, \quad E[n_k^2] = R_k$$

$$E[n_k w_l] = 0 \quad \text{for all values of k and l}$$

TABLE 2

Results of System Noise Sensitivity Analysis

	No filter/Averaging Estimation		Kalman filter/WLS Estimation	
control method	AP	PI	AP	PI
rms conc error	1.43	2.36	1.39	1.59
average conc	99.74	100.84	99.61	100.02

TABLE 3

Results of Airflow Measurements

	Measured Airflow Rate/Enclosure Volume hr^{-1}	
	Low Flow	High Flow
CCTG	1.81	4.30
Decay	1.88	4.32
Orifice	1.90	*

* instrument not operational

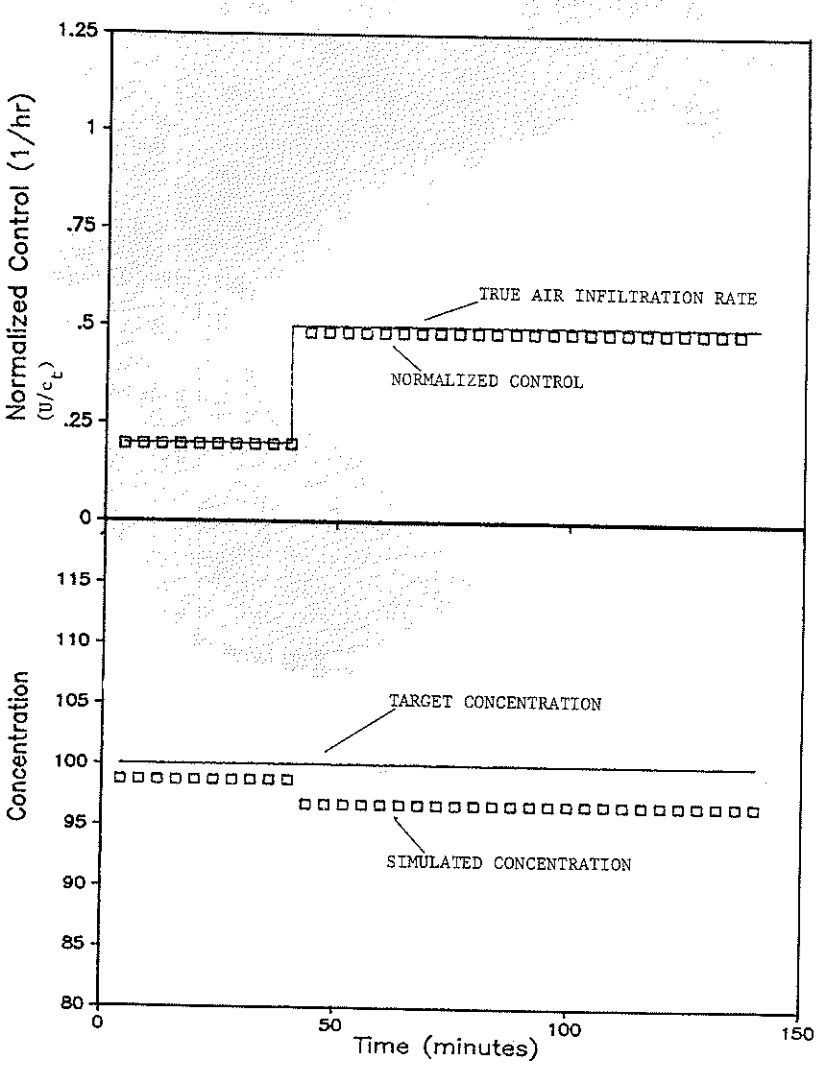

Figure 1. Proportional control: Kp = a/b, pole = 0.0, step change in air (0.2 - 0.5 1/h)

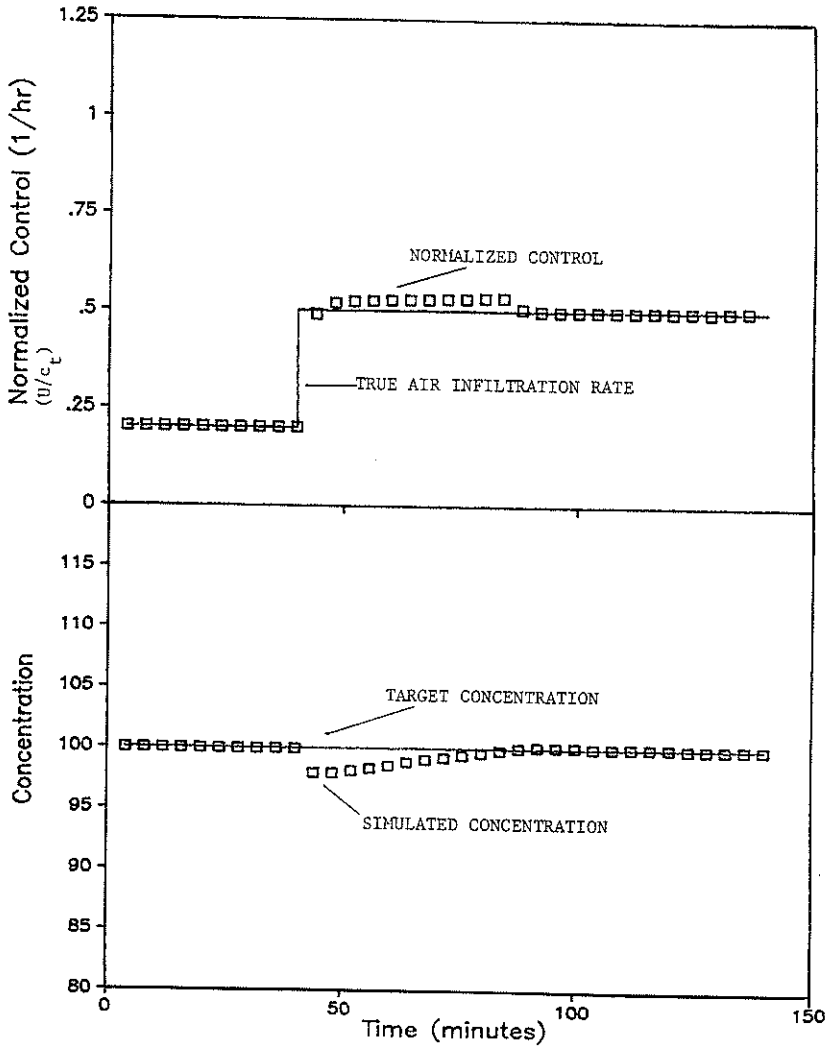

Figure 2. Proportional adaptive control: Kp = a/b, Co = Ct/a, using estimated value of AIR (averaging method)

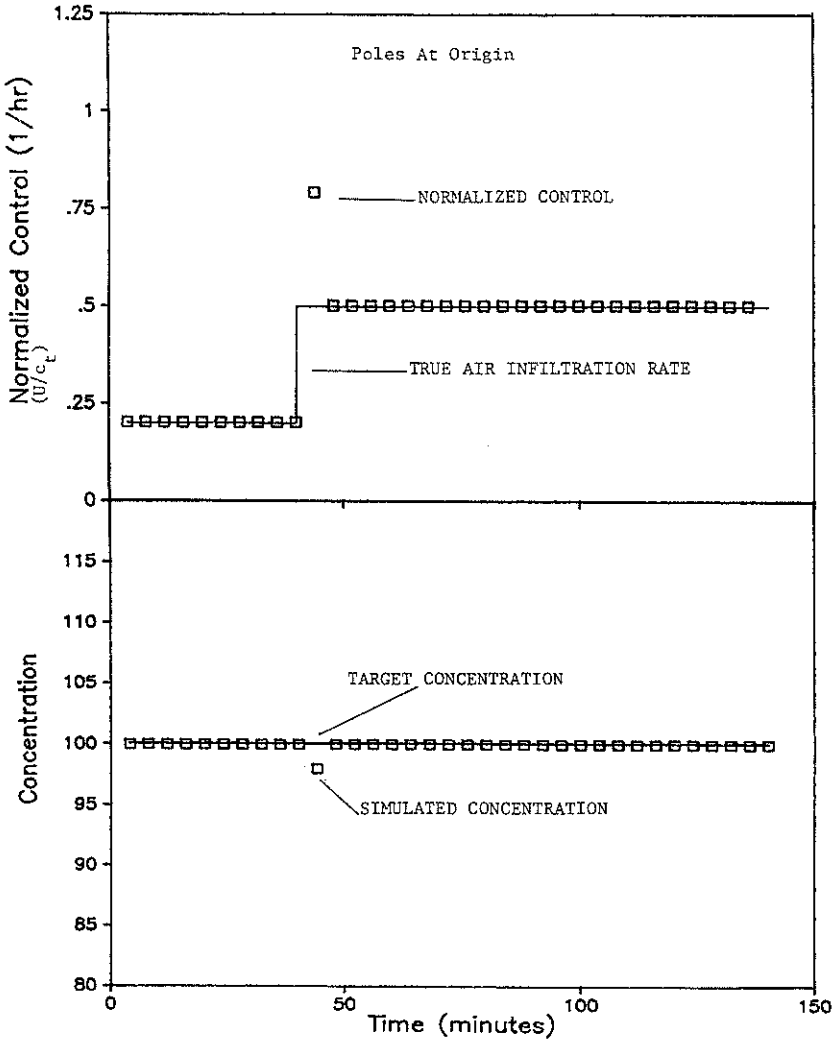

Figure 3. PI control: Kp = a/b, Ki = 1/bTs, step change in air (0.2 -0.5 1/h)

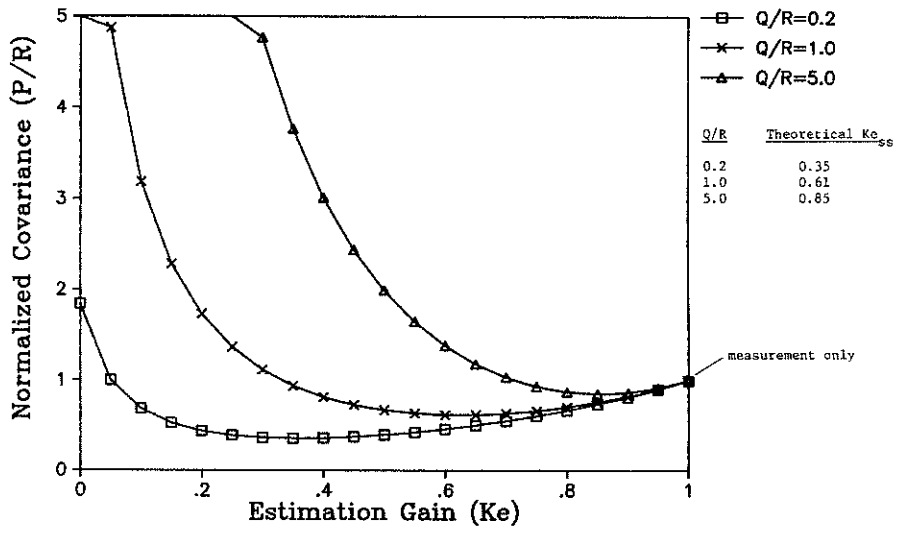

Figure 4. Sensitivity of P to variation in Ke, actual value of AIR used to computed a, b

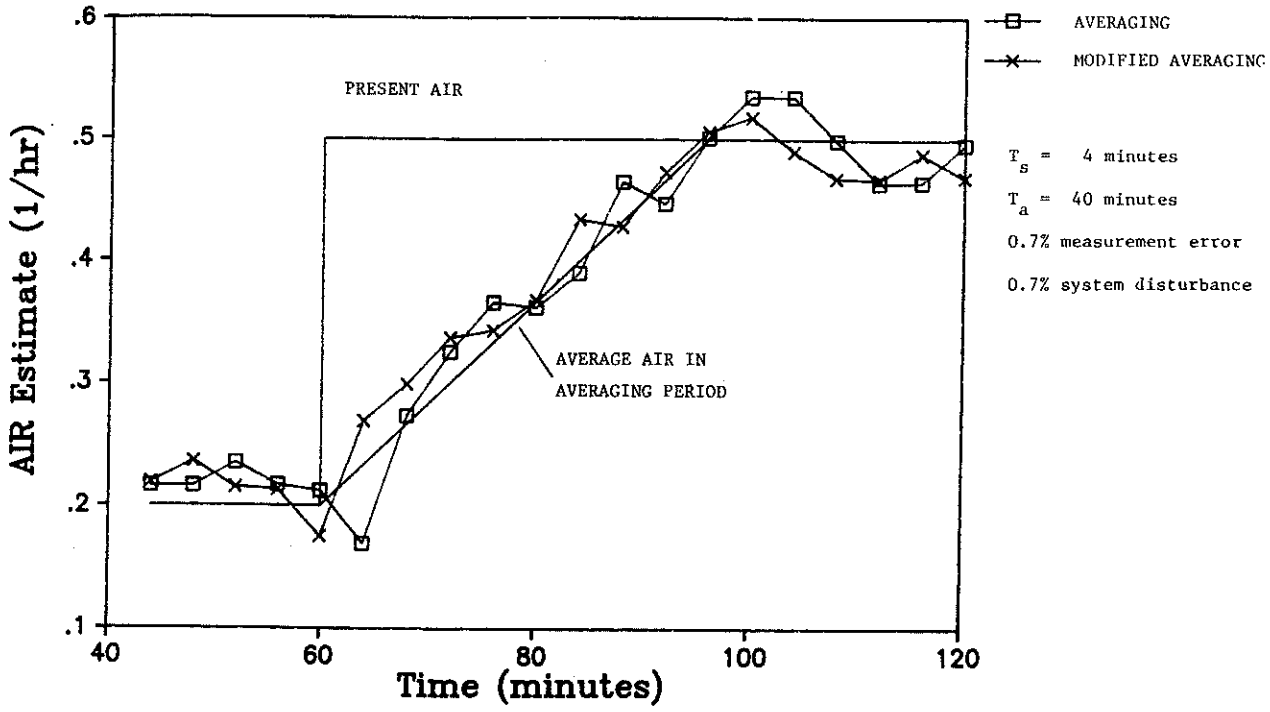

Figure 5. Simulation of AIR estimation for averaging and modified averaging

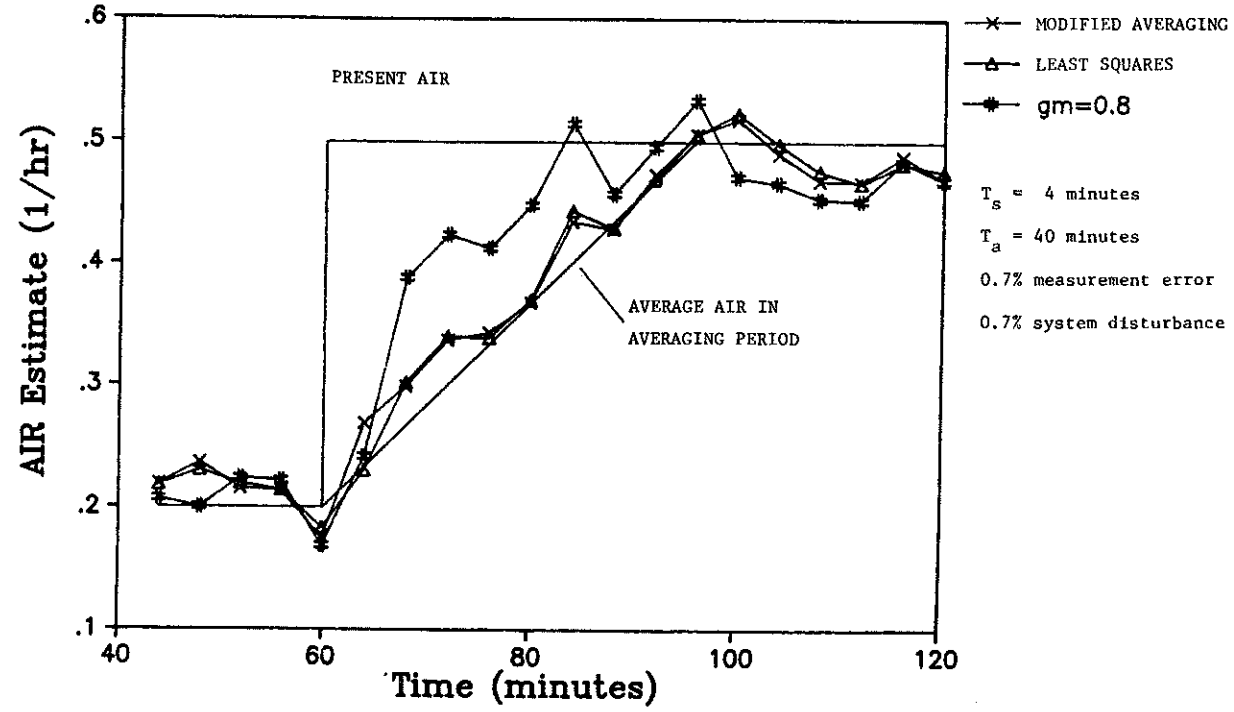

Figure 6. Simulation of AIR estimation for averaging and least squares method

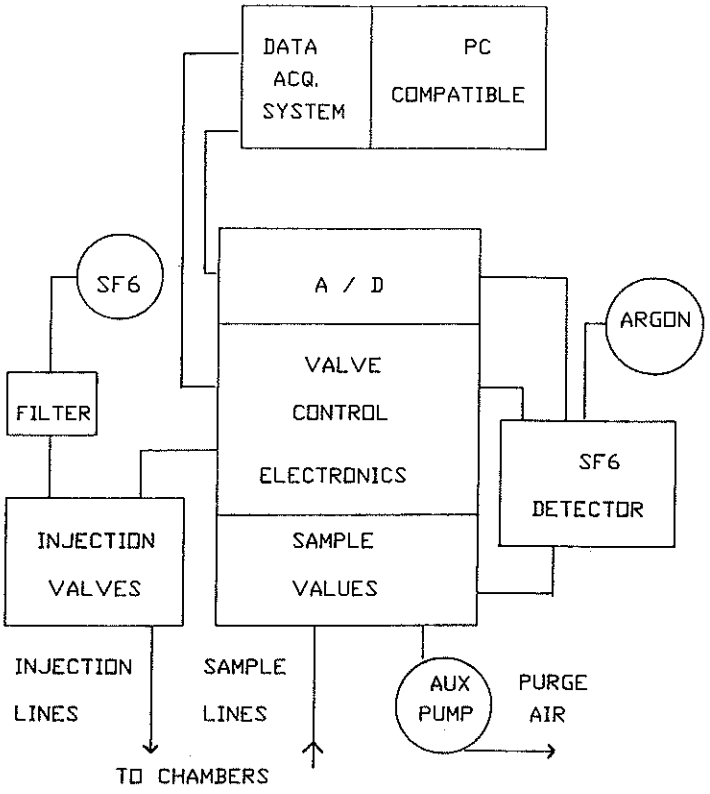

Figure 7. Constant concentration system

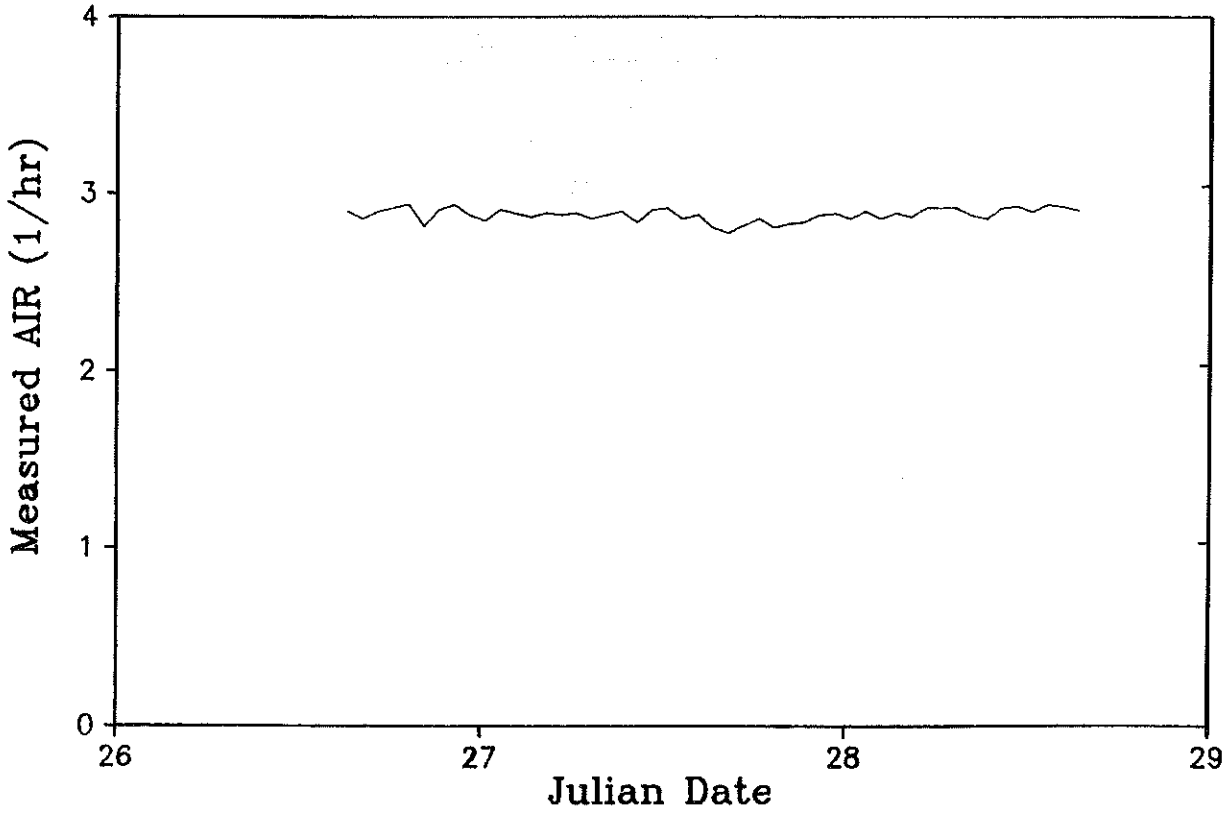

Figure 8. CCTG system drift over two days

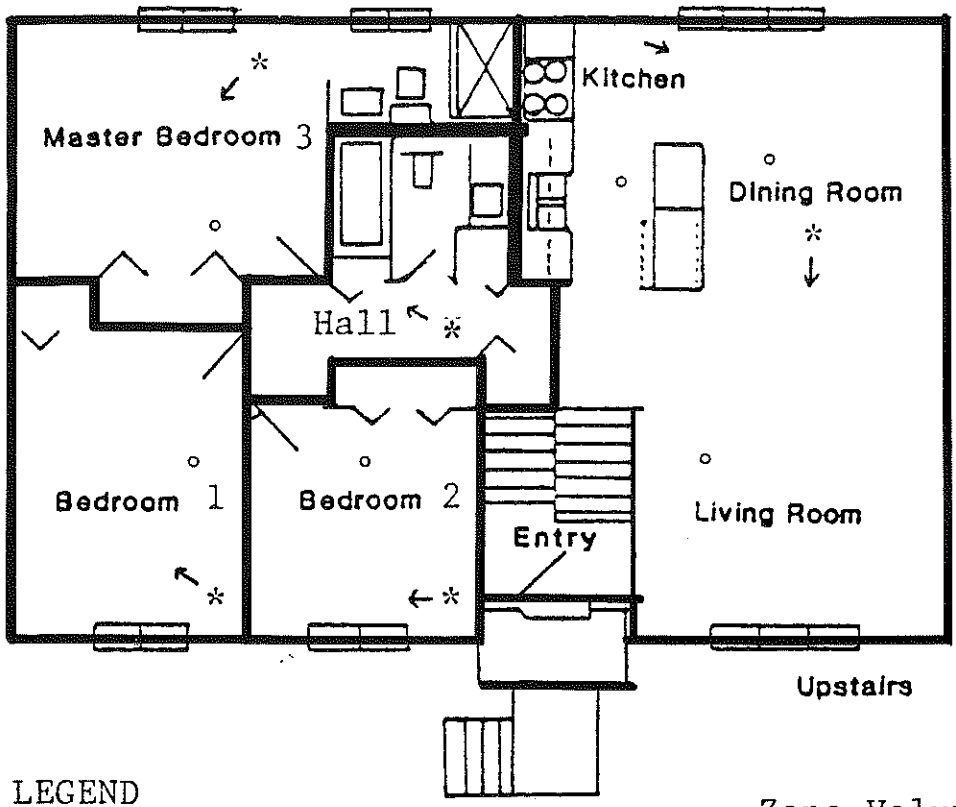

LEGEND

* - Injection Point
° - Sample Point
↑ - Fan Flow

Zone Volume (m^3)	
Bedroom 1	28
Bedroom 2	21
Bedroom 3	39
Hall & Bath	20
Kitch & L/D	83
Basement	121

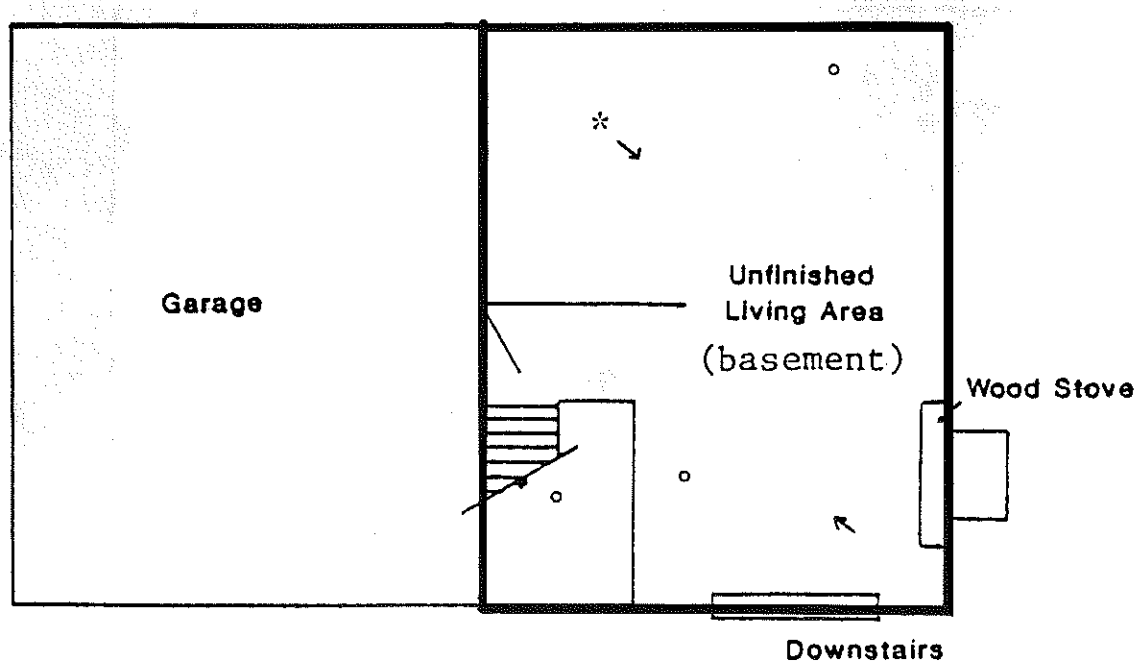

Figure 9. Test house floor plan

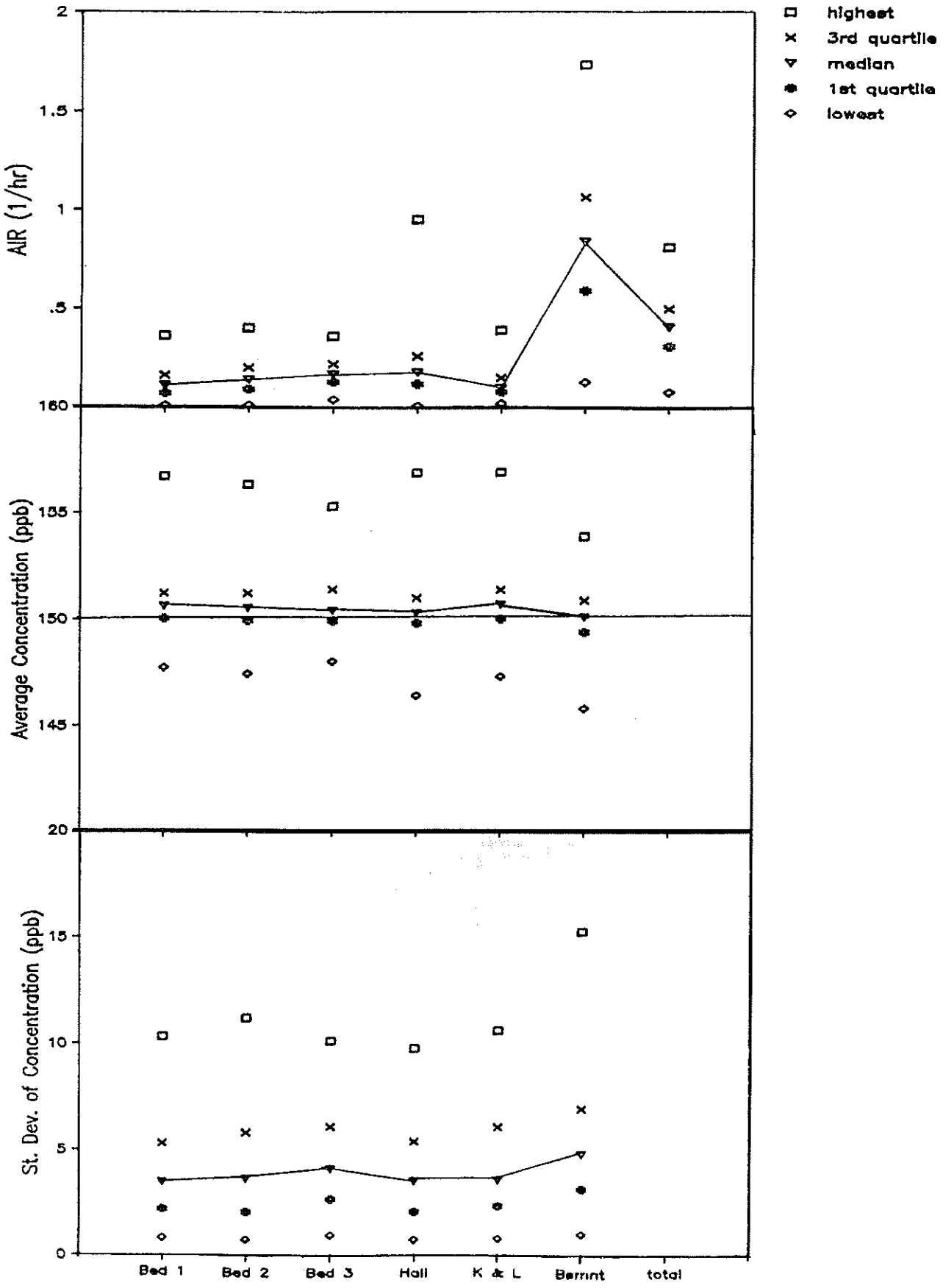

Figure 10. Distribution of hourly data: AIR, average, and standard deviation of concentration

Measurement Method	Fan Operation	Environmental Conditions: Outdoor Temp(°F)	Environmental Conditions: Wind Speed(mph)	Infiltration Rate(1/h)
CCTG	Periodic	49.6 ±0.6	4.7 ±0.5	0.42 ±0.02 0.12 ±0.02 0.90 ±0.02
Decay	Periodic	49.5 ±10.4	4.6 ±3.5	0.47 ±0.23 0.36 ±0.13 0.66 ±0.41
CCTG	Constant	63.9 ±1.8	4.2 ±0.3	0.31 ±0.02 0.21 ±0.03 0.46 ±0.04
Decay	Constant	59.9 ±11.2	4.1 ±2.0	0.30 ±0.12 0.30 ±0.12 0.30 ±0.11

LEGEND

Whole House

Upstairs

Downstairs

Figure 11. Effect of fan operation on infiltration rate measurements

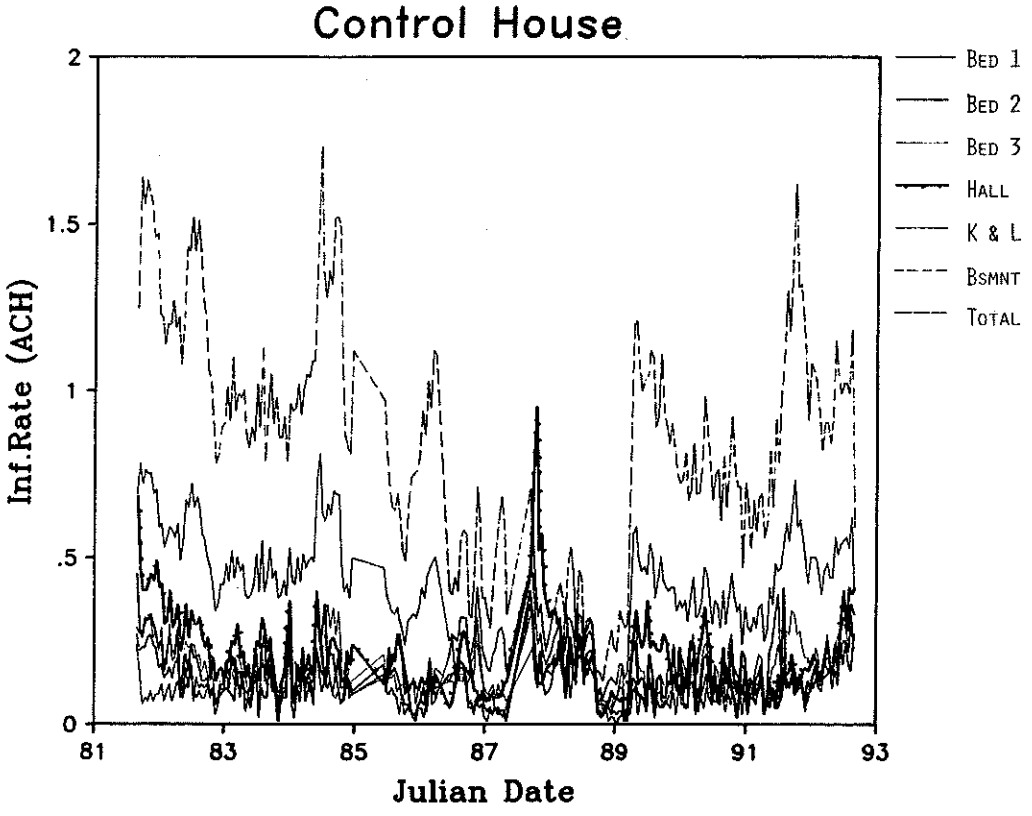

Figure 12

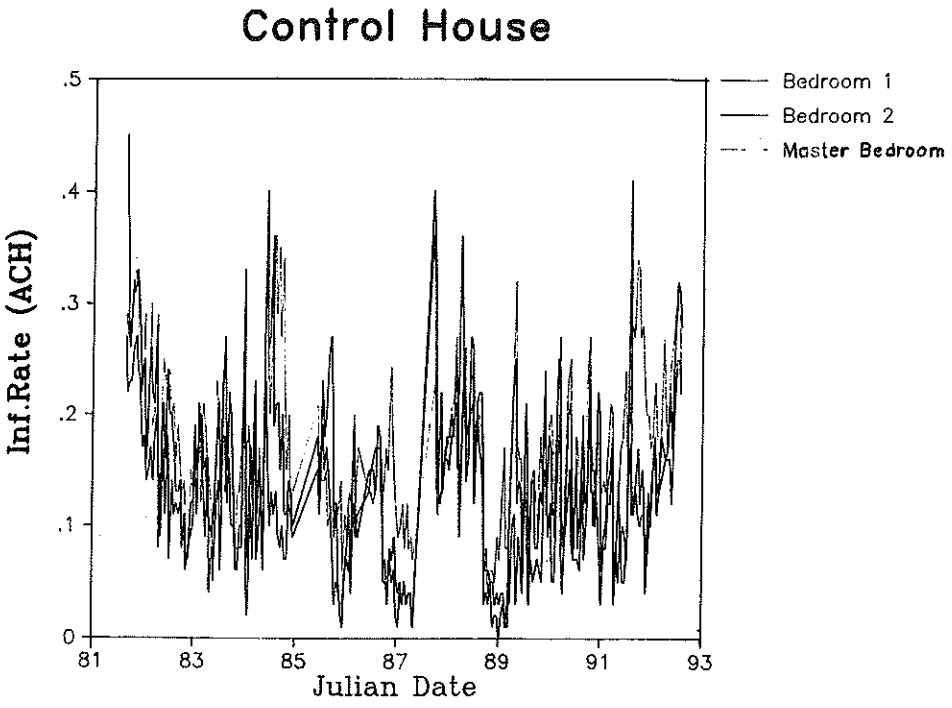

Figure 13

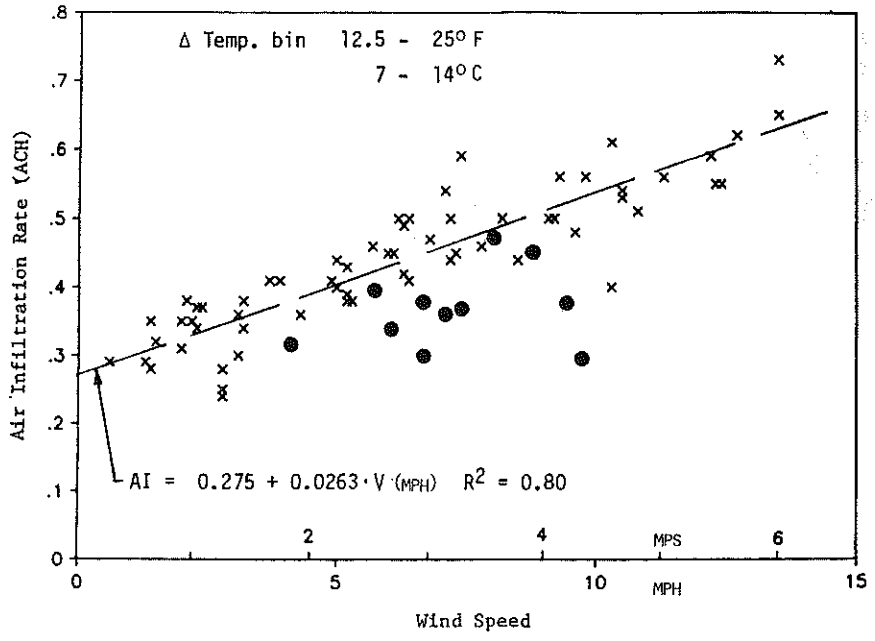

Figure 14. Binned temperature data showing the relationship of wind speed and air infiltration rate for wind direction: ●, wind from "protected" direction; x, all other wind directions